Electrocardiographic and Histopathological Characterizations of Diabetic Cardiomyopathy in Rats

Mahmoud E. Youssef
Delta University for Science and Technology
Mona F. El-Azab
Suez Canal University Faculty of Pharmacy
Marwa A. Abdel-Dayem
Horus University
Galal Yahya Metwally (galalmetwally2020@gmail.com)
Zagazig University Faculty of Pharmacy https://orcid.org/0000-0002-9466-7863
Ibtesam S. Alanazi
UoHB: University of Hafr Al Batin
Sameh Saber
Delta University for Science and Technology

Research Article

Keywords: diabetic complications, cardiomyopathy, electrocardiograph, streptozotocin, troponin.

Posted Date: September 27th, 2021

DOI: https://doi.org/10.21203/rs.3.rs-880567/v1

Version of Record: A version of this preprint was published at Environmental Science and Pollution Research on November 30th, 2021. See the published version at https://doi.org/10.1007/s11356-021-17831-6.

Abstract

Diabetes is a clinical condition that is associated with insulin deficiency and hyperglycemia. Cardiomyopathy, retinopathy, neuropathy, and nephropathy are well known complications of the elevated blood glucose. Diabetic cardiomyopathy is a clinical disorder that is associated with systolic and diastolic dysfunction along with cardiac fibrosis, inflammation, and elevated oxidative stress. In this study, diabetes was induced by intraperitoneal injection of streptozotocin (STZ) 50 mg/kg. We determined the plasma levels of cardiac troponin-T (cTnT), and creatinine kinase MB (CK-MB) by ELISA. Diabetic rats showed abnormal cardiac architecture and increased collagen production. significant elevation in ST-segment, prolonged QRS and QT-intervals, and increased ventricular rate were detected. Additionally, diabetic rats showed a prolongation in P wave duration and atrial tachyarrhythmia was observed. Plasma levels of cTnT and CK-MB were elevated. In conclusion, these electrocardiographic changes (elevated ST-segment, prolonged QT interval, and QRS complex, and increased heart rate) along with histopathological changes and increased collagen formation could be markers for the development of diabetic cardiomyopathy in rats.

1. Introduction

The defect in insulin formation and release leads to diabetes mellitus, which is characterized by an elevation in blood glucose levels. Several pathogenetic processes set behind the progressive damage of beta cells (Cerf 2013) and depletion in insulin secretion or manifestation of insulin resistance in diabetic patients. Prolonged hyperglycemia leads to macrovascular and microvascular damage leading to several complication, including retinopathy, nephropathy, neuropathy, and cardiomyopathy (Cole &Florez 2020). Additionally, development of cardiovascular complications such as ischemic heart disease, peripheral vascular disorder, and stroke is related to microvascular complications (Panari &M 2016).

In diabetic cardiomyopathy, the progression of cardiac fibrosis would induce dysfunctions of the cardiac cycle that can progress to heart failure (Jia et al. 2018). Additional various metabolic disorders are accompanied with diabetic cardiomyopathy such as diminished nitric oxide levels, elevated oxidative stress, inflammation, and enhanced activity of renin-aldosterone angiotensin system (Tan et al. 2020). The occurrence of diabetic cardiomyopathy is linked to several pathophysiological pathways, including the formation of advanced glycation end-products (AGEs), disturbances in microRNA, O-linked-N-acetylglucosamine and exosome (O-GlcNAc) pathways (Ducheix et al. 2018), adenosine monophosphate (AMP)-activated protein kinase (AMPK) (Sun et al. 2020), protein kinase C (PKC) (Yin et al. 2019), and nuclear factor kappa B (NF-κB) formation (Fan et al. 2018).

In diabetes, damage-associated molecular pattern molecules (DAMPs) formation triggers toll-like receptor 4 (TL4)/ NF-κB signaling that promotes high yield of pro-inflammatory cytokines such as interleukin-6 (IL-6) and tumor necrosis factor α (TNF- α) (El-Gizawy et al. 2020, Nasr et al. 2021, Saber 2018). These inflammatory cytokines derive the progress of cardiac dysfunction in diabetic heart. Moreover, the enhanced formation of NF-κB due to stimulation of TLR4 or excessive release of reactive oxygen species

(ROS) could stimulate fibrotic changes and collagen formation through enhancing the activity of tissue growth factor β (TGF-β), which could lead to diabetic cardiomyopathy (Khalil et al. 2020, Saber 2018). This study is aimed to investigate the electrocardiographic and histopathological changes associated with diabetic cardiomyopathy in rats.

2. Materials And Methods

2.1. Animal manipulation

Male Wistar rats with an average weight (175–220 g) and 1 year age were supplied from the animal facility of the Faculty of Pharmacy, Delta University for Science and Technology, Egypt. Animal manipulation, feeding and housing conditions were conducted according to (Youssef et al. 2021). All experiments were performed following the approval of the Experimental Animal Ethics Committee of Suez Canal University No.: 201807PHDA1.

2.2. Chemicals and test kits

Streptozotocin (STZ), used in the induction of type-1 diabetes, was purchased from Sigma-Aldrich (St. Louis, MO, USA). Tetrahydrofuran (THF) was purchased from El-Gomhouria Company for Trading Chemicals and Medical Appliances (Cairo, Egypt) and were used for inhalation anesthesia. cTnT, CK-MB, TNF-α, and IL-6 were measured by ELISA using specific kits obtained from Cusabio Technology LLC (Houston, TX, USA). Primary monoclonal antibodies that were used for the immunostaining of NF-κB were bought from Affinity Biosciences Inc (Changzhou, China). The EnVision™ FLEX immunohistochemistry detection kit was purchased from Dako Inc. (Glostrup, Denmark).

2.3. Experimental approach

Freshly prepared STZ (50 mg/kg) was injected intraperitoneally for the induction of type I diabetes (Raj et al. 2012). Plasma glucose level was detected in the fourth day. Rats were considered diabetic if plasma glucose level is > 250 mg/dL (n = 7). Additional 7 healthy normal rats served as corresponding control groups. The diabetic nor the normal groups received any treatment. Body weight was measured at the beginning of the experiment before STZ injection. It was measured every four days throughout the study period.

2.4. Electrocardiography monitoring

At the end of the experiment (45 days), electrocardiography (ECG) charts were recorded. Animal were anesthetized using THF inhalation and located in supine position after full anesthesia. Electrodes were fixed subcutaneously in the animal's paws and were connected to Kaden Yasen™ ECG-903 device (Zhuhai City, Guangdong, China). The Lead II ECG traces were recorded to analyze P wave anomalies, QT interval, QRS interval, ST-segment elevation, and ventricular rate.

2.5. Collection of plasma

At the end of the experiment, animals were anesthetized by THF inhalation and blood samples were collected form orbital sinus using a sterile capillary tube that were inserted into the eye inner canthus under light anesthesia. Blood samples were collected in EDTA precoated tubes then immediately centrifuged at 5000 rpm /12 minutes. The supernatant was separated in stored at -80° C.

2.6. Evaluation of heart weight changes

Animals were sacrificed, the heart were surgically isolated, excess blood were removed and weighted. For the calculation of heart weight to body weight ratio, the following formula were applied: [heart weight (g)/body weight (g)]. Left and right ventricles were separated by the incision of the atrioventricular septum. The isolated ventricles were cut transversely into two portions. The first portion was immediately stored at -80° C and were used for the preparation of cardiac tissue homogenate. The second portion was fixed in 4% neutral buffered formalin solution, then embedded in paraffin for immunohistochemical and histopathological studies.

2.7. Histopathological examination

Paraffin-embedded section were cut in 4 µm slices and stained with Hematoxylin and eosin (H&E). sections were evaluated using a light microscope (Optika B-352A, BG, Italia) for the detection of histopathological anomalies at 400X magnification (Saber et al. 2020). Additionally, ventricular dilatation and cardiac wall thickness were measured. The following histopathological scoring was applied: 0 (absence of histopathological anomalies); 1 (mild; cardiomyocytes degeneration with slight infiltration of inflammatory cells); 2 (moderate to extensive cardiomyocyte degeneration with diffuse inflammatory cells infiltration); and 3 (severe; necrotic tissue with massive inflammatory cells infiltration) (Joukar et al. 2010). The degree of cardiac tissue damage was determined by examining 20 randomly chosen fields for each group.

2.8. Determination of cTnT, CK-MB, IL-6, and TNF-α levels

Plasma levels of the tested markers were detected by ELISA technique following the manufacturer's protocol. Standard, control, and test samples were placed to ELISA plate precoated with monoclonal antibodies specific for the tested immunogens. The conjugates of both markers were added to each well then 1 hour incubation at room temperature followed by adding the color substrate. After 30 minutes incubation, the enzymatic reactions yielded a blue color that was converted into yellow color after the addition of stop solution. Microplate reader was used for the measurement of optical density.

2.9. Statistical analysis

All data were analyzed using GraphPad Prism 6 software (GraphPad Software, San Diego, CA). Data were expressed as mean ± standard deviation (SD). Means of both groups were compared using unpaired t-test.

3. Results

3.1. body weight and heart weight to body weight ratio

Body weight of diabetic animals were reduced throughout the study period after injection with STZ (Fig. 1a, 1b). In contrary, the body weight of normal untreated rats was continuously increasing. Additionally, the reported drop in the body weight was displayed in the calculated percentage of body weight change. Furthermore, the ratio of heart weight to body weight was significantly elevated in the diabetic group confirming the progression to cardiomegaly (Fig. 1c).

3.2. ECG recordings

The diabetic rats displayed significant increase of ventricular rate compared to the healthy group. (Fig. 2a, 2b). Moreover, additional ECG anomalies were detected such as increased QT interval, increased corrected QT intervals (QTc), and elevation in QRS interval (Fig. 2a, 2c, 2d, 2e). Similarly, the duration of P wave of diabetic rats was significantly prolonged (Fig. 2a, 2g). Regarding the elevation of ST-segment elevation, a consistent increase in the ST-segment elevation was scored compared to the normal group (Fig. 2a, 2f), and trial tachyarrhythmias was observed in diabetic rats (Fig. 2a).

3.3. Ventricular dilatation and ventricular wall thickness

The diabetic group showed a notable dilatation in the left ventricle compared to the normal group indicating the occurrence of diabetic cardiomyopathy (Fig. 3a, 3b). Regarding the ventricular wall thickness, a significant decrease the ventricular wall thickness was clearly observed in diabetic rats relative to control group (Fig. 3a, 3d). In contrary, the dilatation of the right ventricle in both groups remained unaffected (Fig. 3a, 3c).

3.4. Histopathological examination

Histopathological examination of left ventricles showed an abnormal architecture and disarray of cardiomyocytes (Fig. 4c, 4d) compared to normal rats (Fig. 4a, 4b). Additionally, enlarged cardiomyocytes with box-shaped nucleus were detected. The cardiac myofibers demonstrated an abundant helical appearance with myofibers arrangement around a fibrous central core (Fig. 4d). The cardiac myofibers were organized in deviant angles or perpendicular arrangement (Fig. 4c), while the myofibers arrangement in normal healthy untreated rats was parallel pattern (Fig. 4a). The diabetic group demonstrated increased histopathological scoring as an indication for these histopathological anomalies and increased infiltration of inflammatory cells (Fig. 4e). Examination of the cardiac vasculature showed an increase in the formation of perivascular fibrosis in diabetic rats (Fig. 4d) compared to the normal group (Fig. 4b).

3.5. Effect on cTnT, CK-MB, IL-6, and TNF-α

High readings of cTnT and CK-MB are indicators of cardiac damage, STZ- treated rats displayed a substantial elevation in both markers compared to untreated group (Fig. 5a, 5b). Similarly, the measurement of cardiac levels of IL-6 and TNF-α, showed significant increase compared to the normal group (Fig. 5c, 5d).

4. Discussion

Diabetes is a major medical issue worldwide. Several complications are linked to diabetes, including nephropathy, retinopathy, neuropathy, and cardiomyopathy. In our study, induction diabetes was conducted by intraperitoneal injection of STZ. The STZ-induced diabetes is not mechanistically understood. However, since STZ is a chemical analogue of glucose, it is permeated in beta cells, inducing a subsequent cytotoxic reaction that generates reactive nitrogen and oxygen species which by turn damage the beta cells that secret the insulin. Diabetes induction leads to loss of weight due to reduced lipogenesis and enhanced utilization of fats as an energy source (Beylot 1996, Garg et al. 2017).

Diabetic cardiomyopathy is usually connected with electrocardiographic, and histopathological abnormalities (Jia et al. 2016). The anatomical signs of diabetic cardiomyopathy are left ventricular dilatation that accompanied with to left ventricular dysfunction in the early diastolic filling with enhanced isovolumetric relaxation duration (Jia et al. 2016). Systolic dysfunction would be followed by symptomatic heart failure (Lee et al. 1997). The cardiac dysfunction is believed to be raised from the stiffness of cardiomyocytes, cardiac fibrosis, and cardiac hypertrophy (Lee et al. 1997). This dysfunction stimulates the sympathetic tone, which leads to an increased activity of sarcoplasmic reticulum by exaggerated stimulation of β-receptors and ryanodine receptors leading to an intensification of Ca^{++} release and ventricular tachycardia (Assis et al. 2019). In Addition, cardiomyopathy can be developed due to inflammatory reactions or cardiac fibrosis (Krejci et al. 2016). The extreme liberation of Ca^{++} ions from the sarcoplasmic reticulum in cardiomyocytes could cause irregular repolarization, which could explain the prolongation in QT and QTc intervals (Paavola et al. 2016). Development of diabetic cardiomyopathy will lead to the formation of left ventricular bundle block, which might result in dyssynchronous activation of the left ventricles. This dysfunction in ventricular conductivity might justify the prolongation of the QRS complex (Akgun et al. 2014). Cardiac dysfunction in the current model progressed to ischemic dilated cardiomyopathy. This could be explained by the observed atrial arrhythmias observed in our study and (Ducas &Ariyarajah 2013). Furthermore, ischemic dilated cardiomyopathy was ensured by an increase in ST-segment elevation. Diabetic cardiomyopathy is a cardiomyopathy that takes place in the absence of notable coronary artery disease (Jia et al. 2018). however, diabetic cardiomyopathy could be accompanied with coronary vascular abnormalities that may affect the coronary blood flow. Decreasing coronary supply and myocardial perfusion will result in impairing the ventricular function which leads to subsequent clinical outcomes (Sandesara et al. 2018). Several structural and functional abnormalities in coronary blood vessels may occur in diabetics; luminal obstruction, infiltration of inflammatory cells and vascular fibrosis as structural changes while functional changes include dysfunction endothelial cells dysfunction, impaired vasorelaxation and vasoconstriction, diminished cardiac perfusion (Sandesara et al. 2018).

The advancement of dilated diabetic cardiomyopathy would stimulate fibrosis, which is considered a familiar marker for cardiomyopathy (Ho et al. 2010). The reduction in adenosine triphosphate (ATP) levels could lead to impaired perfusion and energetics of cardiomyocytes. This would result in reduced cardiac functionality, in addition to microvascular abnormalities (Raman et al. 2019). The modified

cardiac functions encourage mutations in the genes encoding myofibers proteins, which may lead to an enhanced fibrosis (Araco et al. 2017).

Many proteins are incorporated in cardiac myofibers contractions. Troponin is one of these proteins. Three complex proteins represent troponin; troponin C, I, and T (Kraus et al. 2018). The detection of cTnT along with CK-MB in plasma is crucial for the diagnosis of cardiac dysfunctions (C.C. et al. 2010). CK enzyme is important for the conversion of creatinine with the assistance of ATP molecules to form phosphocreatine and adenosine diphosphate (ADP) (Bessman &Carpenter 1985). CK is differentiated into three isoforms that are distributed in different body tissues. CK-MB is mainly found in cardiac muscles, CK-MM is expressed in skeletal muscles and CK-BB, the brain CK isoform (Schlattner et al. 2006). The damage of CK-rich tissue will lead to high CK levels detected in plasma (Schlattner et al. 2006). Therefore, detection of cTnT and CK-MB in plasma could be used for the diagnosis of cardiomyopathy, as was previously described by other clinical (Ali et al. 2016, Odum &Young 2018) and animal studies (Al-Rasheed et al. 2017).

NF-κB is believed to regulate inflammatory reactions by enhancing the production of pro-inflammatory cytokines such as IL-6, TNF-α, and IL-1β (Gianello et al. 2019, Saber et al. 2019a, Zhai et al. 2020). This inflammatory response is quick, as NF-κB is previously stored inactivated form in the cytoplasm. Moreover, activated NF-κB stimulates cardiac hypertrophy and fibrosis (Nakamura &Sadoshima 2018). Diabetes is always coupled with elevated ROS activity and stimulation of the renin-angiotensin-aldosterone system, which results in the subsequent increase in NF-κB formation and excess of pro-inflammatory cytokines (Jia et al. 2016, Saber et al. 2019b, Thomas et al. 2014). These mediators are responsible for the quick progression of diabetic cardiomyopathy (Ali et al. 2020, Yu et al. 2003). The elevated levels of TNF-α and IL-6 could impair the capability of cardiomyocytes to handle the Ca^{++} ions through lowering the sarcoplasmic/endoplasmic reticulum Ca^{++} ATPase production (Villegas et al. 2000). This was previously shown in type I model of diabetes induced by STZ in mice, where IL-6 knock out lessened the progress of diabetic cardiomyopathy and enhanced cardiac function (Zhang et al. 2016). Moreover, NF-κB activation increased the release of ROS (Saber et al. 2021), which could be due to the increased activity of nicotinamide adenine dinucleotide phosphate (NADPH) oxidase (Mariappan et al. 2010). Pyrrolidine dithiocarbamate derived inhibition of NF-κB restored cardiac function in diabetic animals and improved the mitochondrial structural integrity and prevented oxidative stress (Mariappan et al. 2010).

5. Conclusion

In conclusion, diabetic cardiomyopathy in rats could be diagnosed with several ECG anomalies, including ST-segment elevation, prolongation of QRS complex and QT interval, and increased ventricular rate. The presence of atrial tachyarrhythmia could be due to atrial dilatation. Moreover, diabetes-induced cardiac injury leads to an elevation in cardiac specific biomarkers such as cTnT and CK-MB. Several histopathological alterations were detected in the hearts of diabetic rats. Cardiac myofibers took the arrangement of perpendicular angles and encircled a fibrotic helical core, which is a substantial

anatomical hallmark of dilated cardiomyopathy. Collagen formations was increased in the perivascular area of the coronary blood vessels with enhanced infiltration of inflammatory cells. Additionally, diabetic cardiomyopathy is correlated with high IL-6, and TNF-α cardiac levels.

Abbreviations

AMP, adenosine monophosphate; AMPK, adenosine monophosphate-activated protein kinase; ATP, adenosine triphosphate; CK-MB, creatinine kinase MB; cTnT, cardiac troponin; DAMPs, damage-associated molecular pattern molecules; ECG, electrocardiography; EDTA, ethylene diamine tetra-acetic acid; IL-6, interleukin-6; NADPH, nicotinamide adenine dinucleotide phosphate; NF-κB, nuclear factor kappa B; ROS, reactive oxygen species; TGF-β, tissue growth factor β; THF, tetrahydrofuran; TLR4, toll-like receptor 4; TNF-α, tumor necrosis factor α.

Declarations

Authors' contributions:

Mahmoud E. Youssef contributed to conception, data acquisition and analysis, manuscript synthesis, histological examinations, image analysis, and data validation.. Mona F. El-Azab, Marwa A. Abdel-Dayem, Galal Yahya, Ibtesam S. Alanazi, contributed to data analysis and discussion, manuscript synthesis. Sameh Saber handled animals, provided software, conducted statistical analysis. All authors have read and approved the manuscript for publication.

Data availability:

The data used in the current study are available from the relevant authors upon reasonable request.

Funding:

Not applicable

Ethics approval and consent to participate:

All experiments were performed following the approval of the Experimental Animal Ethics Committee of Suez Canal University No.: 201807PHDA1.

Consent for publication:

Not applicable.

Acknowledgments:

Not applicable.

Conflicts of Interest:

The authors declare that there is no conflict of interests

References

1. Akgun T, Kalkan S, Tigen MK (2014) Variations of QRS Morphology in Patients with Dilated Cardiomyopathy; Clinical and Prognostic Implications. Journal of cardiovascular and thoracic research 6, 85 – 9
2. Al-Rasheed NM, Al-Rasheed NM, Hasan IH, Al-Amin MA, Al-Ajmi HN, Mohamad RA, Mahmoud AM (2017) Simvastatin Ameliorates Diabetic Cardiomyopathy by Attenuating Oxidative Stress and Inflammation in Rats. Oxidative medicine and cellular longevity 2017, 1092015
3. Ali, Naqvi SA, Bismillah M, Wajid N (2016) Comparative analysis of biochemical parameters in diabetic and non-diabetic acute myocardial infarction patients. Indian heart journal 68, 325 – 31
4. Ali, Abo-Salem OM, El Esawy BH, El Askary A (2020) The Potential Protective Effects of Diosmin on Streptozotocin-Induced Diabetic Cardiomyopathy in Rats. Am J Med Sci 359:32–41
5. Araco M, Merlo M, Carr-White G, Sinagra G (2017) Genetic bases of dilated cardiomyopathy. Journal of cardiovascular medicine 18:123–130
6. Assis FR, Krishnan A, Zhou X, James CA, Murray B, Tichnell C, Berger R, Calkins H, Tandri H, Mandal K (2019) Cardiac sympathectomy for refractory ventricular tachycardia in arrhythmogenic right ventricular cardiomyopathy. Heart rhythm 16:1003–1010
7. Bessman SP, Carpenter CL (1985) The creatine-creatine phosphate energy shuttle. Annual review of biochemistry 54, 831 – 62
8. Beylot M (1996) Regulation of in vivo ketogenesis: role of free fatty acids and control by epinephrine, thyroid hormones, insulin and glucagon. Diabetes Metab 22:299–304
9. M CC, I. A PEJ (2010) Diabinese and Nicotinic acid Combination Reduced Cardiovascular Indices in Experimental Diabetes. Asian J Research Chem 3:785–790
10. Cerf M (2013) Beta Cell Dysfunction and Insulin Resistance. Frontiers in endocrinology 4
11. Cole JB, Florez JC (2020) Genetics of diabetes mellitus and diabetes complications. Nat Rev Nephrol 16:377–390
12. Ducas R, Ariyarajah V (2013) Atrial Fibrillation in Patients with Ischemic and Non-Ischemic Left Ventricular Dysfunction. Journal of atrial fibrillation 5:535
13. Ducheix S, Magre J, Cariou B, Prieur X (2018) Chronic O-GlcNAcylation and Diabetic Cardiomyopathy: The Bitterness of Glucose. Front Endocrinol 9:642
14. El-Gizawy SA, Nouh A, Saber S, Kira AY (2020) Deferoxamine-loaded transfersomes accelerates healing of pressure ulcers in streptozotocin-induced diabetic rats. Journal of Drug Delivery Science Technology 58:101732

15. Fan L, Xiao Q, Zhang L, Wang X, Huang Q, Li S, Zhao X, Li Z (2018) CAPE-pNO2 attenuates diabetic cardiomyopathy through the NOX4/NF-kappaB pathway in STZ-induced diabetic mice. Biomedicine pharmacotherapy = Biomedecine pharmacotherapie 108:1640–1650
16. Garg M, Ghanim H, Kuhadiya ND, Green K, Hejna J, Abuaysheh S, Torre B, Batra M, Makdissi A, Chaudhuri A, Dandona P (2017) Liraglutide acutely suppresses glucagon, lipolysis and ketogenesis in type 1 diabetes. Diabetes Obes Metab 19:1306–1311
17. Gianello V, Salvi V, Parola C, Moretto N, Facchinetti F, Civelli M, Villetti G, Bosisio D, Sozzani S (2019) The PDE4 inhibitor CHF6001 modulates pro-inflammatory cytokines, chemokines and Th1- and Th17-polarizing cytokines in human dendritic cells. Biochem Pharmacol 163:371–380
18. Ho CY, Lopez B, Coelho-Filho OR, Lakdawala NK, Cirino AL, Jarolim P, Kwong R, Gonzalez A, Colan SD, Seidman JG, Diez J, Seidman CE (2010) Myocardial fibrosis as an early manifestation of hypertrophic cardiomyopathy. The New England journal of medicine 363, 552 – 63
19. Jia G, DeMarco VG, Sowers JR (2016) Insulin resistance and hyperinsulinaemia in diabetic cardiomyopathy. Nature reviews. Endocrinology 12, 144 – 53
20. Jia G, Hill MA, Sowers JR (2018) Diabetic Cardiomyopathy: An Update of Mechanisms Contributing to This Clinical Entity. Circ Res 122:624–638
21. Joukar S, Najafipour H, Khaksari M, Sepehri G, Shahrokhi N, Dabiri S, Gholamhoseinian A, Hasanzadeh S (2010) The effect of saffron consumption on biochemical and histopathological heart indices of rats with myocardial infarction. Cardiovasc Toxicol 10:66–71
22. Khalil R, Shata A, Abd El-Kader EM, Sharaf H, Abdo WS, Amin NA, Saber S (2020) Vildagliptin, a DPP-4 inhibitor, attenuates carbon tetrachloride-induced liver fibrosis by targeting ERK1/2, p38α, and NF-κB signaling. Toxicol Appl Pharmacol 407:115246
23. Kraus D, von Jeinsen B, Tzikas S, Palapies L, Zeller T, Bickel C, Fette G, Lackner KJ, Drechsler C, Neumann JT, Baldus S, Blankenberg S, Munzel T, Wanner C, Zeiher AM, Keller T (2018) Cardiac Troponins for the Diagnosis of Acute Myocardial Infarction in Chronic Kidney Disease. Journal of the American Heart Association 7:e008032
24. Krejci J, Mlejnek D, Sochorova D, Nemec P (2016) Inflammatory Cardiomyopathy: A Current View on the Pathophysiology, Diagnosis, and Treatment. BioMed research international 2016, 4087632
25. Lee M, Gardin JM, Lynch JC, Smith VE, Tracy RP, Savage PJ, Szklo M, Ward BJ (1997) Diabetes mellitus and echocardiographic left ventricular function in free-living elderly men and women: The Cardiovascular Health Study. American heart journal 133:36–43
26. Mariappan N, Elks CM, Sriramula S, Guggilam A, Liu Z, Borkhsenious O, Francis J (2010) NF-kappaB-induced oxidative stress contributes to mitochondrial and cardiac dysfunction in type II diabetes. Cardiovascular research 85, 473 – 83
27. Nakamura M, Sadoshima J (2018) Mechanisms of physiological and pathological cardiac hypertrophy. Nat Rev Cardiol 15:387–407
28. Nasr M, Almawash S, Al Saqr A, Bazeed AY, Saber S, Elagamy HI (2021) Bioavailability and Antidiabetic Activity of Gliclazide-Loaded Cubosomal Nanoparticles. Pharmaceuticals 14

29. Odum EP, Young EE (2018) Elevated cardiac troponin I, creatine kinase and myoglobin and their relationship with cardiovascular risk factors in patients with type 2 diabetes. Diabetes metabolic syndrome 12:141–145
30. Paavola J, Vaananen H, Larsson K, Penttinen K, Toivonen L, Kontula K, Laine M, Aalto-Setala K, Swan H, Viitasalo M (2016) Slowed depolarization and irregular repolarization in catecholaminergic polymorphic ventricular tachycardia: a study from cellular Ca2 + transients and action potentials to clinical monophasic action potentials and electrocardiography. Europace: European pacing, arrhythmias, and cardiac electrophysiology : journal of the working groups on cardiac pacing, arrhythmias, and cardiac cellular electrophysiology of the European Society of Cardiology 18, 1599–1607
31. Panari H, M V (2016) Study on Complications of Diabetes Mellitus among the Diabetic Patients. Asian J Nur Edu Research 6:171–182
32. Raj SM, Mohammed S, S VK, C SK, Debnath S (2012) Antidiabetic Effect of Luffa acutangula Fruits and Histology of Organs in Streptozotocin Induced Diabetic in Rats. Research J Pharmacognosy Phytochemistry 4:64–69
33. Raman B, Ariga R, Spartera M, Sivalokanathan S, Chan K, Dass S, Petersen SE, Daniels MJ, Francis J, Smillie R, Lewandowski AJ, Ohuma EO, Rodgers C, Kramer CM, Mahmod M, Watkins H, Neubauer S (2019) Progression of myocardial fibrosis in hypertrophic cardiomyopathy: mechanisms and clinical implications. Eur Heart J Cardiovasc Imaging 20:157–167
34. Saber S (2018) Angiotensin II: a key mediator in the development of liver fibrosis and cancer. Bulletin of the National Research Centre 42:18
35. Saber S, Khodir AE, Soliman WE, Salama MM, Abdo WS, Elsaeed B, Nader K, Abdelnasser A, Megahed N, Basuony M, Shawky A, Mahmoud M, Medhat R, Eldin AS (2019a) Telmisartan attenuates N-nitrosodiethylamine-induced hepatocellular carcinoma in mice by modulating the NF-kappaB-TAK1-ERK1/2 axis in the context of PPARgamma agonistic activity. Naunyn Schmiedebergs Arch Pharmacol 392:1591–1604
36. Saber S, Khodir AE, Soliman WE, Salama MM, Abdo WS, Elsaeed B, Nader K, Abdelnasser A, Megahed N, Basuony M, Shawky A, Mahmoud M, Medhat R, Eldin AS (2019b) Telmisartan attenuates N-nitrosodiethylamine-induced hepatocellular carcinoma in mice by modulating the NF-κB-TAK1-ERK1/2 axis in the context of PPARγ agonistic activity. Naunyn Schmiedebergs Arch Pharmacol 392:1591–1604
37. Saber S, Abd El-Kader EM, Sharaf H, El-Shamy R, El-Saeed B, Mostafa A, Ezzat D, Shata A (2020) Celastrol augments sensitivity of NLRP3 to CP-456773 by modulating HSP-90 and inducing autophagy in dextran sodium sulphate-induced colitis in rats. Toxicol Appl Pharmacol 400:115075
38. Saber S, Youssef ME, Sharaf H, Amin NA, El-Shedody R, Aboutouk FH, El-Galeel YA, El-Hefnawy A, Shabaka D, Khalifa A, Saleh RA, Osama D, El-Zoghby G, Gobba NA (2021) BBG enhances OLT1177-induced NLRP3 inflammasome inactivation by targeting P2X7R/NLRP3 and MyD88/NF-κB signaling in DSS-induced colitis in rats. Life Sci 270:119123

39. Sandesara PB, O'Neal WT, Kelli HM, Samman-Tahhan A, Hammadah M, Quyyumi AA, Sperling LS (2018) The Prognostic Significance of Diabetes and Microvascular Complications in Patients With Heart Failure With Preserved Ejection Fraction. Diabetes Care 41:150–155
40. Schlattner U, Tokarska-Schlattner M, Wallimann T (2006) Mitochondrial creatine kinase in human health and disease. Biochim Biophys Acta 1762:164–180
41. Sun Y, Zhou S, Guo H, Zhang J, Ma T, Zheng Y, Zhang Z, Cai L (2020) Protective effects of sulforaphane on type 2 diabetes-induced cardiomyopathy via AMPK-mediated activation of lipid metabolic pathways and NRF2 function. Metab Clin Exp 102:154002
42. Tan Y, Zhang Z, Zheng C, Wintergerst KA, Keller BB, Cai L (2020) Mechanisms of diabetic cardiomyopathy and potential therapeutic strategies: preclinical and clinical evidence. Nature reviews, Cardiology
43. Thomas CM, Yong QC, Rosa RM, Seqqat R, Gopal S, Casarini DE, Jones WK, Gupta S, Baker KM, Kumar R (2014) Cardiac-specific suppression of NF-kappaB signaling prevents diabetic cardiomyopathy via inhibition of the renin-angiotensin system. Am J Physiol Heart Circ Physiol 307:H1036–H1045
44. Villegas S, Villarreal FJ, Dillmann WH (2000) Leukemia Inhibitory Factor and Interleukin-6 downregulate sarcoplasmic reticulum Ca2 + ATPase (SERCA2) in cardiac myocytes. Basic Res Cardiol 95:47–54
45. Yin L, Fang Y, Song T, Lv D, Wang Z, Zhu L, Zhao Z, Yin X (2019) FBXL10 regulates cardiac dysfunction in diabetic cardiomyopathy via the PKC beta2 pathway. J Cell Mol Med 23:2558–2567
46. Yu, Kennedy RH, Liu SJ (2003) JAK2/STAT3, not ERK1/2, mediates interleukin-6-induced activation of inducible nitric-oxide synthase and decrease in contractility of adult ventricular myocytes. J Biol Chem 278:16304–16309
47. Youssef ME, Abdelrazek HM, Moustafa YM (2021) Cardioprotective role of GTS-21 by attenuating the TLR4/NF-κB pathway in streptozotocin-induced diabetic cardiomyopathy in rats. Naunyn-Schmiedeberg's Arch Pharmacol 394(1):11–31. doi:10.1007/s00210-020-01957-4
48. Zhai Y, Zhu Y, Liu J, Xie K, Yu J, Yu L, Deng H (2020) Dexmedetomidine Post-Conditioning Alleviates Cerebral Ischemia-Reperfusion Injury in Rats by Inhibiting High Mobility Group Protein B1 Group (HMGB1)/Toll-Like Receptor 4 (TLR4)/Nuclear Factor kappa B (NF-kappaB) Signaling Pathway. Medical science monitor: international medical journal of experimental and clinical research 26, e918617
49. Zhang, Wang JH, Zhang YY, Wang YZ, Wang J, Zhao Y, Jin XX, Xue GL, Li PH, Sun YL, Huang QH, Song XT, Zhang ZR, Gao X, Yang BF, Du ZM, Pan ZW (2016) Deletion of interleukin-6 alleviated interstitial fibrosis in streptozotocin-induced diabetic cardiomyopathy of mice through affecting TGFbeta1 and miR-29 pathways. Scientific reports 6:23010

Figures

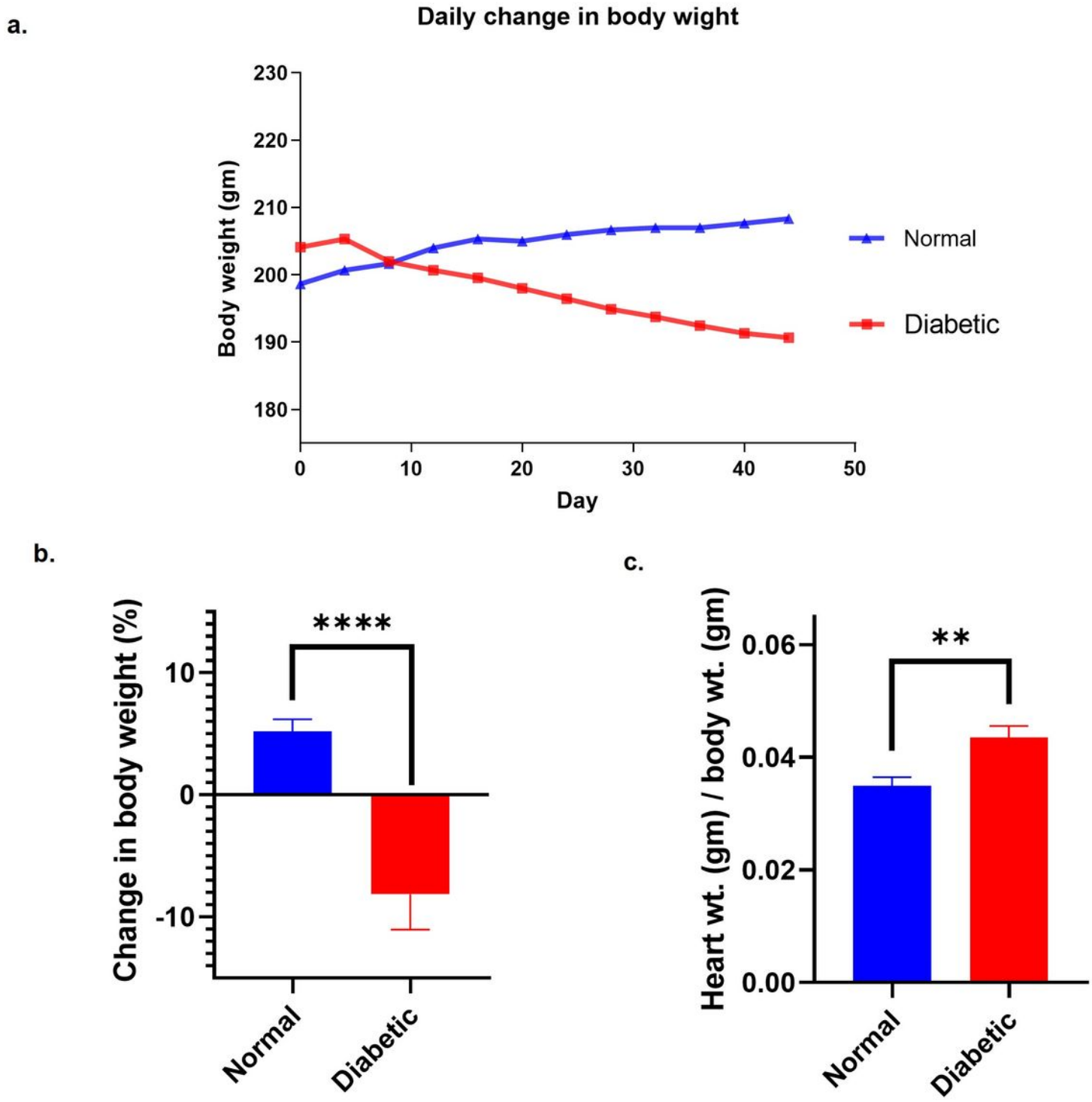

Figure 1

Changes in body weight and heart-to-body weight ratio a. Effect on body weight. b. effect on percentage change in body weight. c. Effect on heart weight to body weight ratio. Data were analyzed using the unpaired t-test with Welch's correction and were expressed as mean ± SD. **** = $P \leq 0.0001$, * = $P \leq 0.05$ with respect to the normal group, (n=7).

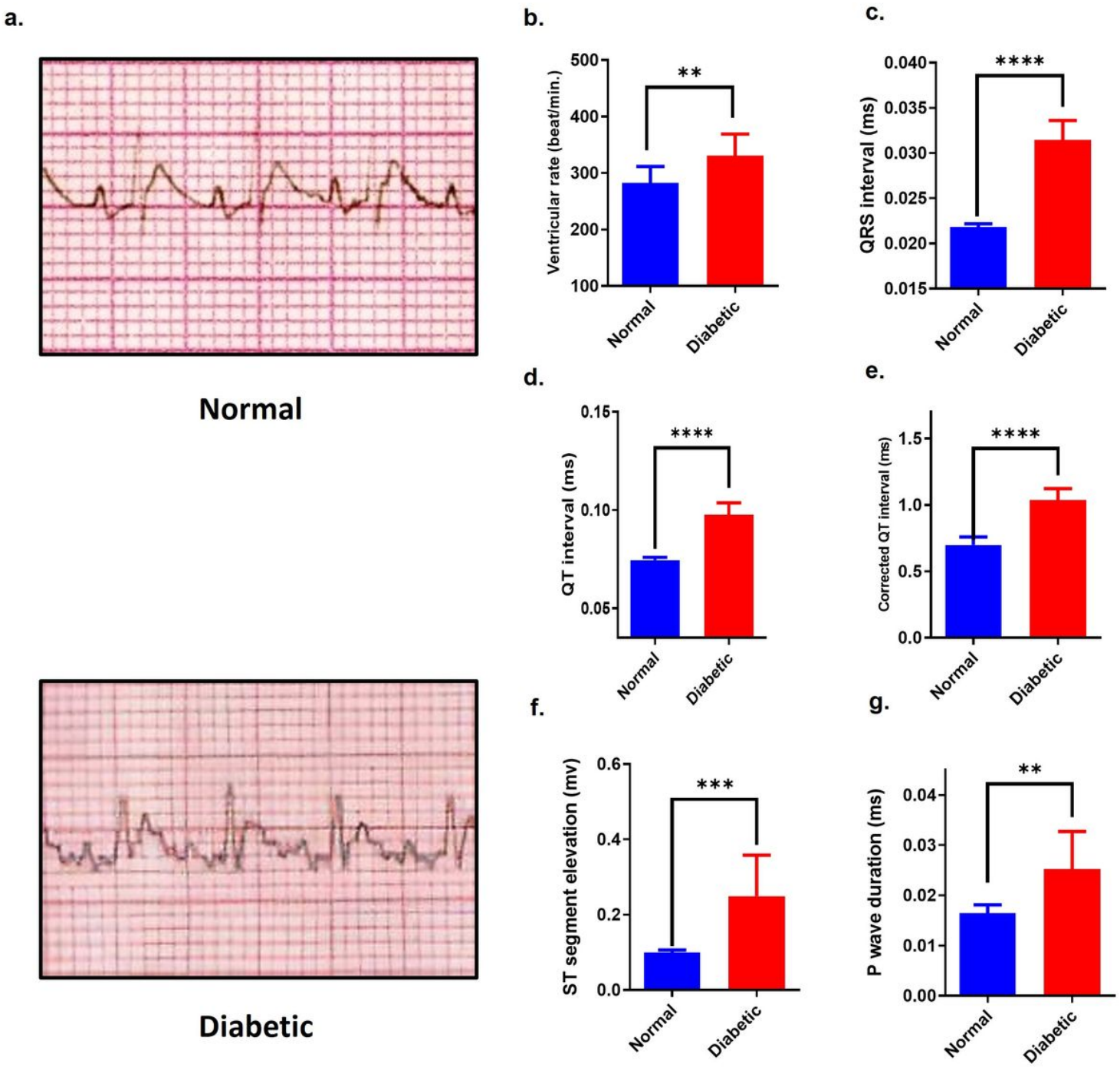

Figure 2

Effect on ECG recordings a. Differential effects on ECG parameters in diabetic rats compared to normal untreated rats. ST segment elevation (blue lines) b. ventricular rate (beat/min). c. QRS interval duration. d. QT interval duration. e. Corrected QT-interval duration. f. ST-segment elevation. g. P wave duration. Data were analyzed using the unpaired t-test with Welch's correction and were expressed as mean ± SD. **** = P≤0.0001, *** = P≤0.001, ** = P≤0.01 and * = P≤0.05 with respect to the normal group, (n=7).

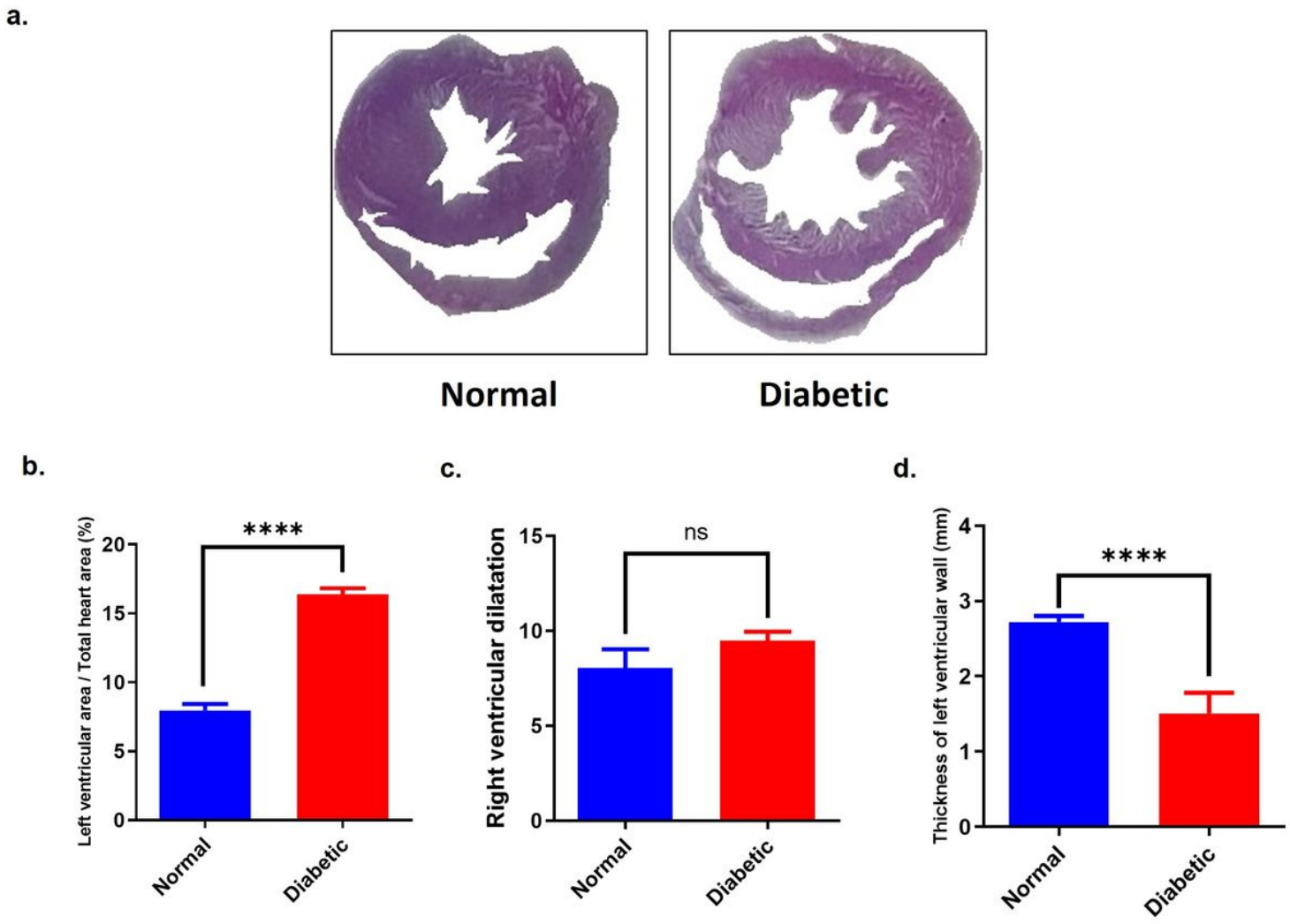

Figure 3

Ventricular dilatation a. Photographic representation of ventricular cardiac sections of different groups. b. Left ventricular dilatation. c. Right ventricular dilatation. d. Left ventricular wall thickness. Data were analyzed using the unpaired t-test with Welch's correction and were expressed as mean ± SD and. **** = P≤0.0001, *** = P≤0.001, ** = P≤0.01 and * = P≤0.05 with respect to the normal group, (n=7).

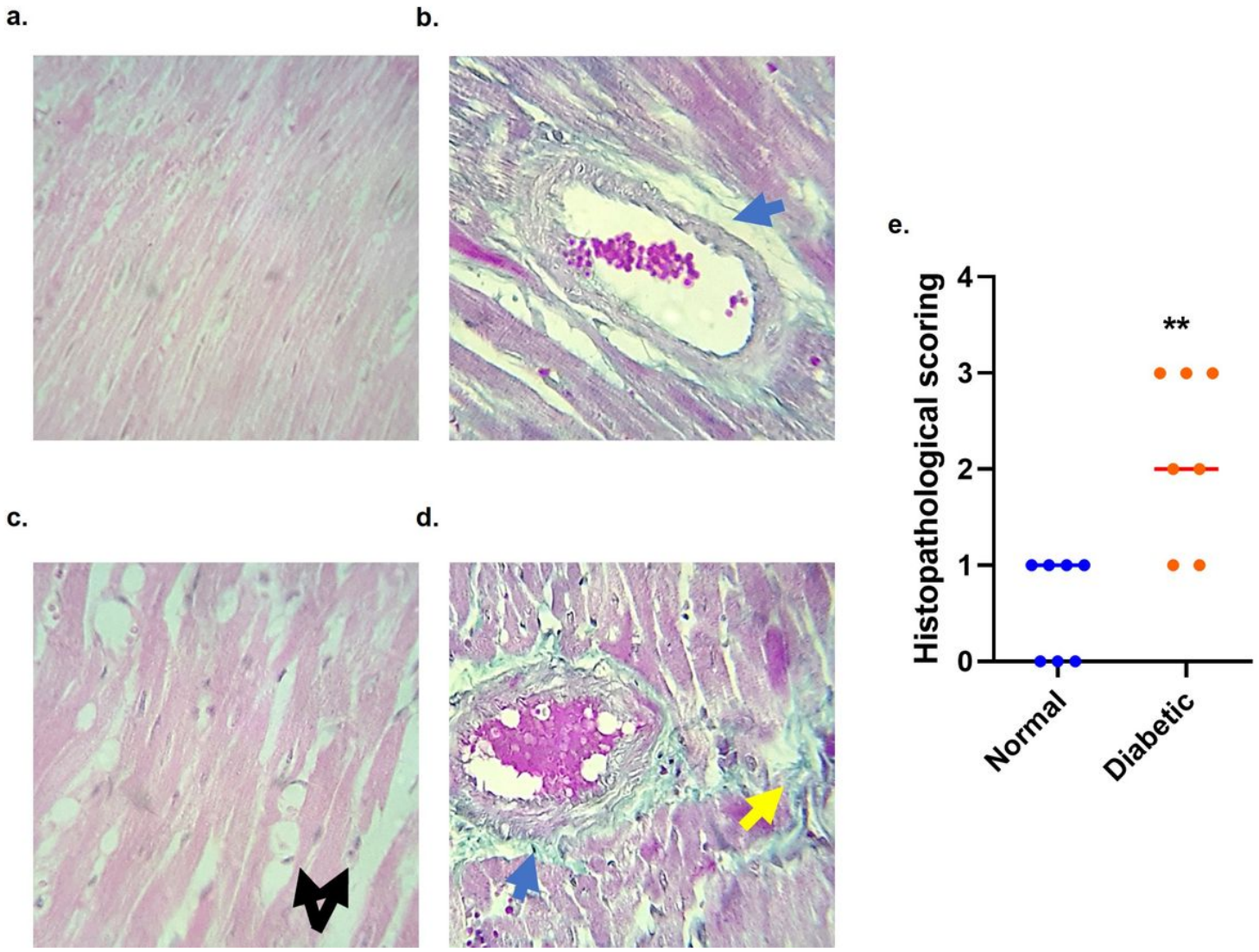

Figure 4

Histopathological examination of cardiac tissue. Photomicrographic representation of heart (400X) a. Normal myofibers architecture in normal group (stained with H&E.). b. Perivascular fibrosis (blue arrow) in the normal group (stained with Masson's trichrome stain). c. Disarray of cardiac myofibers in the diabetic group (stained with H&E) with infiltration of inflammatory cells (black arrow). d. perivascular fibrosis (blue arrow) of the diabetic group (stained with Masson's trichrome stain). It shows a helical arrangement of cardiac myofibers (yellow arrow). e. Histopathological scoring. Data were analyzed using the unpaired t-test with Welch's correction and were expressed as mean ± SD and. **** = P≤0.0001, *** = P≤0.001, ** = P≤0.01 and * = P≤0.05 with respect to the normal group, (n=7).

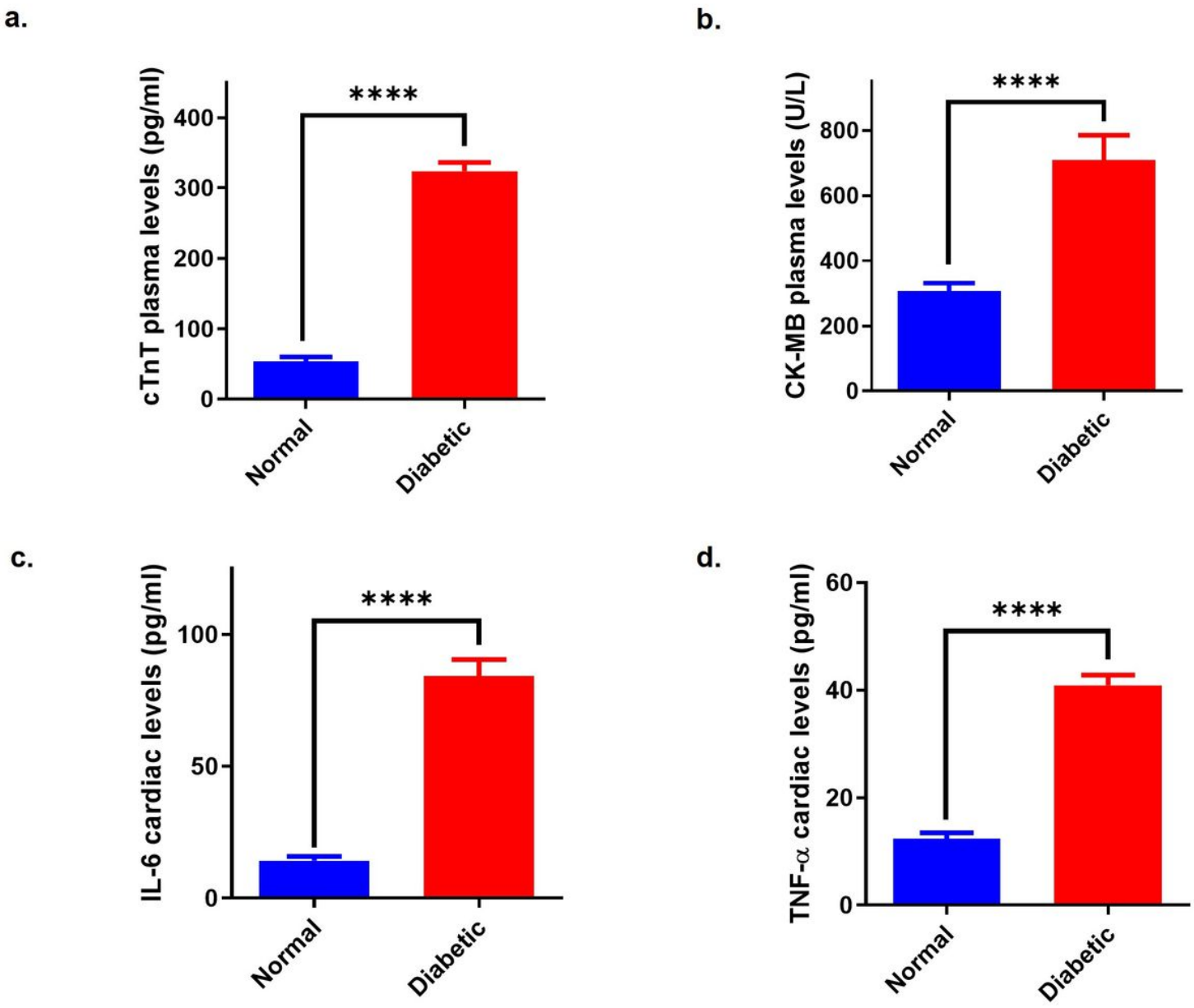

Figure 5

cTnT, CK-MB, IL-6, and TNF-α levels a. Plasma levels of cTnT. b. Plasma levels of CK-MB. c. IL-6 in the cardiac levels. d. TNF-α in the cardiac levels. Data were analyzed using the unpaired t-test with Welch's correction and were expressed as mean ± SD and. **** = P≤0.0001, *** = P≤0.001, ** = P≤0.01 and * = P≤0.05 with respect to the normal group, (n=7).